Fundamentals of Mass Transfer and Kinetics
for the Hydrogenation of Nitrobenzene to Aniline

Reinaldo M. Machado, Air Products and Chemicals, Inc.

No. 01-2007

The catalytic hydrogenation of nitrobenzene to aniline in a continuously mixed slurry reactor is a complex chemical process. A number of competing mass transfer and kinetic rate processes contribute to the overall observed reaction rate. Scale-up and optimization of the process require that the contributing rate processes are understood individually and their impact on the total process is quantified. Laboratory reactors must be operated under conditions that will allow meaningful process characterization and scale-up.

Two classical mechanistic routes to aniline from nitrobenzene are possible depending upon process conditions and the effects of gas/liquid and liquid/catalyst mass transfer. Intermediates formed during these competing chemical routes can act as catalyst poisons that can radically change reactor performance.
This paper will describe and characterize these competing processes for scale-up.

Keywords: Mass transfer, kinetics, scale-up, hydrogenation, aniline, nitrobenzene, slurry, agitation, liquid-solid, catalyst, pulse kinetics, reaction rate.

Introduction

From a historical perspective, aniline is perhaps one of the more important synthetic organic chemicals ever manufactured. In 1856, Sir William Henry Perkin, a student at the Royal College of Chemistry in London, discovered and isolated a purple dye during the oxidation of impure aniline[1]. The discovery of this dye, known as mauve, created quite a stir and Perkin, seeing the value of his discovery, proceeded to scale up the synthetic process for the production of mauve, which included the synthesis of aniline. This process was to become one of the first commercial processes to generate a synthetic organic chemical.

During the last three decades, polyurethane plastics have emerged as a growth industry and aniline once again plays a key role as an industrial intermediate used in the manufacture of MDI, 4,4'-diphenylmethane diisocyanate, a key commercial monomer in the manufacture of polyurethane plastics.

Aniline is produced by the reduction of nitrobenzene, which is produced from the nitration of benzene in a mixture of sulfuric and nitric acid. Originally, nitrobenzene was reacted with dispersed iron in the presence of HCl to generate aniline and an iron oxide sludge.

$$\text{C}_6\text{H}_5\text{NO}_2 + 9/4\ \text{Fe} + \text{H}_2\text{O} \xrightarrow{\text{HCl}} \text{C}_6\text{H}_5\text{NH}_2 + 3/4\ \text{Fe}_3\text{O}_4 \quad (1)$$

This process generated large quantities of waste and was eventually replaced by the catalytic hydrogenation of nitrobenzene in a three-phase slurry reactor.

METTLER TOLEDO

Aniline can also be produced in the gas phase by the reduction of nitrobenzene with hydrogen over fixed catalysts[2]. This paper focuses on the characterization of a slurry process for the reduction of nitrobenzene to aniline.

$$\text{C}_6\text{H}_5\text{NO}_2 + 3\ \text{H}_2 \xrightarrow{\text{Catalyst}} \text{C}_6\text{H}_5\text{NH}_2 + 2\ \text{H}_2\text{O} \qquad (2)$$

The catalytic hydrogenation of nitrobenzene to aniline in a continuously mixed slurry reactor is a complex chemical process.
A number of competing mass transfer and kinetic rate processes contribute to the overall observed reaction rate. Scale-up and optimization of the process require that the contributing rate processes are understood individually and that their impact on the total process rate be quantified. Laboratory reactors must be operated under conditions that will allow meaningful process characterization for scale-up.

The key rate processes are illustrated in Figure 1, which shows schematically typical concentration profiles during the hydrogenation of the nitrobenzene: first, the rate of hydrogen mass transfer from the gas phase to the liquid phase; the rate of hydrogen and nitrobenzene mass transfer from the bulk liquid phase to the outer surface of the catalyst; the rate of hydrogen and nitrobenzene mass transfer into the porous catalyst; and finally, the adsorption and kinetic rates of the hydrogen and nitrobenzene on the inner catalytic surface of the catalyst particle.

Two classical, mechanistic pathways to aniline from nitrobenzene are possible depending upon process conditions and the effects of gas/liquid and liquid/catalyst mass transfer. Intermediates formed during these competing chemical routes can act as reversible catalyst poisons that can radically change reactor performance. It is not within the scope of this paper to exhaustively review the literature or to optimize the process catalysts, temperature or conditions for the reduction of nitrobenzene to aniline; rather, this paper will describe the principles, laboratory methods and analysis techniques for characterizing these competing processes.
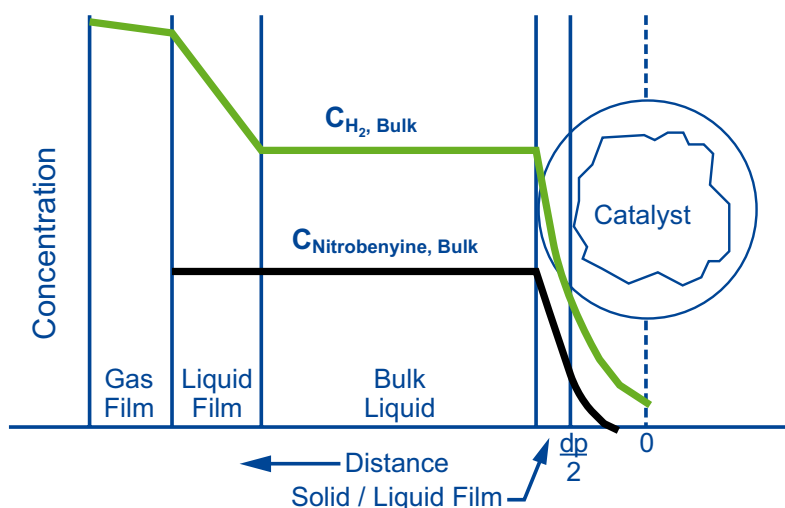

Figure 1
Typical concentration profile during hydrogenation of nitrobenzene.

Literature
A review of the literature can yield a confusing description of the overall process kinetics of nitrobenzene hydrogenation with authors reporting reaction orders for nitrobenzene and hydrogen between zero and one depending upon reaction conditions[3-6].
A general review of the kinetic studies is given in the doctoral thesis by Füsun Yücelen[7]. Most kinetic studies generate global kinetic rate models based on hydrogen uptake and overall conversion. However some detailed studies using analytical methods to identify the individual intermediate species have also been used to characterize reaction kinetic processes[8].

Additionally, most of the kinetics studies in the literature are conducted at relatively low temperatures with solvents. Optimized industrial processes would rather eliminate the use of solvents and their associated separation processes, which can negatively impact overall process economics. Environmental pressures also tend to favor processes that use fewer solvents.

It would generally be preferred to use the reaction products of the nitrobenzene reduction, i.e., aniline and water, as the reaction solvent. Unfortunately, aniline and water are not miscible at low temperatures; therefore, higher temperatures must be employed to maintain a single liquid phase under process conditions. No literature studies are reported under these conditions. It is hoped that his study will help shed some light on this process while illustrating the general principles required for characterizing a hydrogenation process from the laboratory scale.

Experimental

For this set of studies the global reaction kinetics was determined by continuously monitoring the reaction exotherm using the METTLER TOLEDO RC1/HP60 high-pressure reactor fitted with a single baffle and gas induction agitator supplied by Mettler-Toledo Inc.[9]. The METTLER TOLEDO PIC10 pressure controller was operated to allow hydrogen gas into the reactor to maintain the desired pressure setpoint while gas was not allowed to exit the reactor.

The reduction of nitrobenzene to aniline is exothermic and generates −536.6 ± 5.9 kJ/mole as measured in this study, making the calorimetric method ideal for this process. Reagents were all purchased through Aldrich. Individual species were monitored using internal standard gas chromatographic methods. Sponge nickel or Raney® type catalysts were used in this study at concentrations between 0.05 % and 0.10 %. All reactions were carried out with the agitator operating at 1000 rpm, which gave a mixing intensity measured at 1.0 watt/liter.

Chemistry

The chemistry for the reduction of nitrobenzene to aniline was originally elucidated by Haber as reported by Strätz[10] and is illustrated in Figure 2.

Two paths exist to aniline according to this scheme. The first proceeds from the sequential reduction of nitrobenzene: first to nitrosobenzene, next to phenylhydroxylamine, and finally to aniline.

This path, we will see, is favored under conditions in which the concentrations of nitrobenzene are low, < 0.15 %. If the concentrations of nitrosobenzene and phenylhydroxylamine are allowed to increase, the formation of azoxybenzene proceeds rapidly followed by reduction to azobenzene, phenyl hydrazine, and finally, aniline.

The second path, while ultimately yielding aniline, is much slower kinetically on nickel catalysts and is favored under conditions in which the nitrobenzene concentrations are high, > 0.15 %. During high temperature studies, the only stable intermediates identified and monitored were nitrobenzene, azoxybenzene and azobenzene, as we will see later.

Aniline/Water Solubility

The solubility of aniline and water has been well documented and is illustrated in Figure 3[11,12].

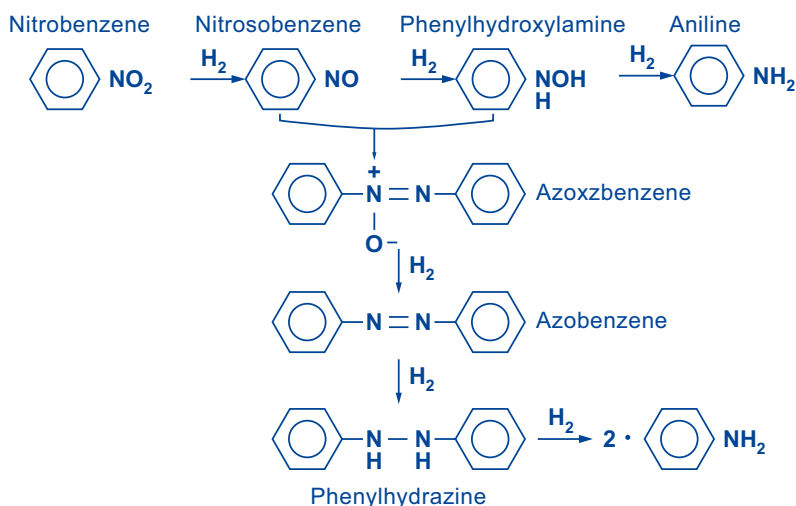The stoichiometric composition of the complete reduction product of nitrobenzene is 27.9 % water/72.1 %

Figure 2
Haber's reaction pathways for the reduction of nitrobenzene to aniline, Strätz[10].
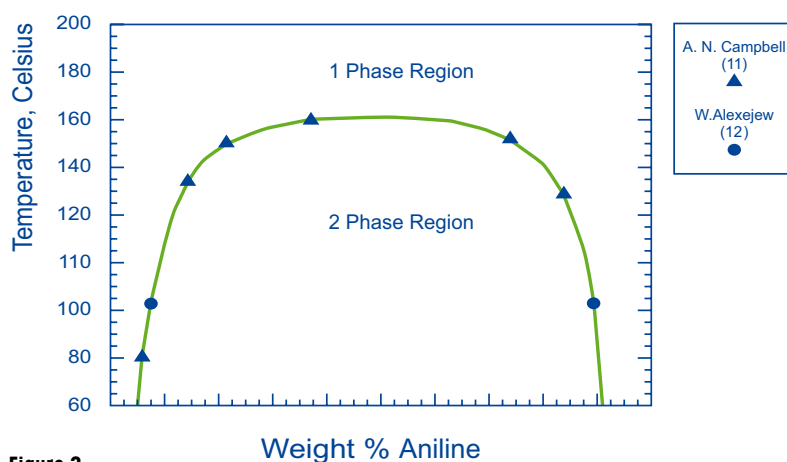

Figure 3
Aniline/water phase diagram.

aniline. From Figure 3, temperatures in excess of 160 °C would be required to keep this mixture homogeneous. High temperatures can impact byproduct chemistry, reducing aniline yields. However, if aniline is fed to the reactor system along with the nitrobenzene or if water is continuously removed via distillation, the concentration of aniline in a continuous process can be maintained at aniline concentrations higher than that dictated by the stoichiometry.

Therefore, lower temperatures are required to keep the system homogeneous. In this study the continuous feed to the reactor consisted of 50 % aniline and 50 % nitrobenzene, which maintained a nominal steady-state composition in the reactor of 14.3 % water and 85.7 % aniline. Under this composition, temperatures in excess of 135 °C are required to maintain homogeneity of the liquid phase.

Gas-Liquid Mass Transfer

The primary and most fundamental rate process that must be characterized when conducting any hydrogenation reaction is the mass transfer of gas into the liquid reaction phase. In most industrial processes using pure hydrogen, the gas film mass transfer resistance can be ignored and mass transfer rates are dominated by the liquid film resistance. The rate of gas mass transfer can then be represented by the following expression:

$$\text{Rate} = \frac{kl \cdot Ag}{V_L \left(C_{H_2,\,sat} - C_{H_2,\,bulk}\right)} \tag{3}$$

where kl = liquid side mass transfer coefficient [m/sec], Ag = gas/liquid interfacial area, VL = reactor liquid volume. The parameters $kl \cdot Ag/VL$ can be combined into the familiar mass transfer coefficient,

$$\frac{kl \cdot Ag}{V_L} = kla \tag{4}$$

The mass transfer coefficient, kla [sec^{-1}], can be viewed as a fundamental parameter describing a particular reactor system. Numerous correlations for the gas mass transfer coefficient in a variety of reactors have been documented[13,14].

However, these correlations may not be applicable to small laboratory reactors that often exhibit unique mixing dynamics and reactor geometry and operate with a particular chemistry and a wide spectrum of process physical properties. Often trying to match performance and mixing between small- and largescale reactors is difficult when only relying upon mechanical measurements such as agitation rate, geometry, agitator design, etc. A more consistent approach to studying process dynamics in small reactors is to measure the gas mass transfer coefficient directly in the actual reaction system. Establishing a realistic mass transfer correlation for the laboratory reactor system will allow «tuning» of the kla to the desired conditions required for the scale-up or scale-down of a process. The strategy for scale-up is to match mass transfer coefficients, kla, from the small to the large scale rather than trying to match geometry, agitation rates, or other mixing characteristics.

Batch Absorption Method for the Determination of kla and Gas Solubility

Numerous techniques have been applied to the measurement of gas-liquid mass transfer in slurry reactors and bubble columns[15-18].

Many involve the oxidation of aqueous sulfite solutions and the absorption of oxygen. Measured values of kla from these experiments must be translated to the system of interest, which requires detailed knowledge of the physical properties of the reaction mixture. An alternative to this method is the use of the batch absorption method, which determines the kla in the exact reaction composition to be used in the process study under the process conditions of interest. The advantages of this approach are obvious as no estimates of physical properties are required and the exact mass transfer coefficient for the system of interest is obtained directly.

Both the gas solubility and the mass transfer coefficient, kla, can be accurately measured for virtually any liquid chemical system by monitoring the batch absorption of a gas into a liquid. This is accomplished by continuously monitoring the pressure drop via a fast-response pressure transducer in a batch gas-liquid system. The technique described by Dietrich et al. is straight forward to implement[19].

First, the volume of the reaction/mass-transfer vessel must be determined. The mass of the liquid and its density at the process temperature must also be known. Next, the reactor is filled approximately half full with the process liquid to be studied without the catalyst. For the solubility measurements to be accurate, the system must be completely purged of all gases so that the only gases in the system are vapors from the liquid phase.

Once the system has been purged, it is sealed and equilibrated at the temperature to be studied with appropriate agitation. The equilibrium pressure of the liquid with its vapor is recorded. Next the agitator rotation is stopped and the circulating liquid in the reactor is allowed to stabilize. The gas to be studied is slowly added to the head space of the reaction vessel to the desired pressure. It is important to preheat the gas to the process temperature before introduction into the vessel. During this entire procedure the temperature and pressure are monitored. The quiescent mixture is allowed to stabilize for 1 or 2 minutes and then the agitation is increased within 1 to 2 seconds to its final designated value. The pressure from a fast-response pressure transducer is monitored electronically and recorded using a fast data sampling device or a strip chart recorder.

Immediately after the agitator is started, the pressure in the vessel begins to decrease as gas from the head space of the reactor vessel is absorbed into the liquid. The pressure continues to drop until the saturation point is reached.

A typical example of this experiment is illustrated in Figure 4. It is clear from Figure 4 that the rate of absorption is strongly influenced by the agitation intensity. From this data both the gas solubility and the mass-transfer coefficient, kla, can be determined. The key results are summarized in the following equations:

$$C_{Lsat} = \left(P - P_E\right) \cdot \frac{P_M - P_E}{P_F - P_{EL}} \cdot \frac{V_G}{V_L} \cdot \frac{1}{RT} \quad (5)$$

$$\ln\left(\frac{P_M - P_F}{P - P_F}\right) = kla \cdot \left(\frac{P_M - P_E}{P_F - P_E}\right) \cdot t \quad (6)$$

$$\ln\left(\alpha\right) = - kla \cdot \left(\frac{P_M - P_E}{P_F - P_E}\right) \cdot t \quad (7)$$

where

C_{Lsat} = saturation solubility of gas in the liquid phase [mole/liter or M],

P = pressure in the vessel [barabs],

P_M = maximum pressure after the head space is charged with gas [barabs],

P_F = final pressure after gas has saturated the liquid phase [barabs],

P_E = equilibrium pressure of the liquid with its vapor [barabs],

V_G = volume of the gas phase [liters],

V_L = volume of the liquid phase [liters],

R = ideal gas constant, 0.08314 [barabs·liter/mole·K],

T = temperature in degrees [K],

kla = mass transfer coefficient [sec^{-1}],

t = time from the onset of agitation [sec],

α = alpha, $(P-P_F)/(P_M-P_F)$, fraction of pressure remaining.

The key assumptions in this analysis are as follows: first, the gas phase is ideal and follows the ideal gas law. Second, the value of kla is constant during the experiment. Finally, the volume of the liquid and gas phases is essentially constant during the experiment. The data illustrated in Figure 4 is plotted according to Equation 7 in Figure 5. From the slope of the line, the value of kla can be determined.
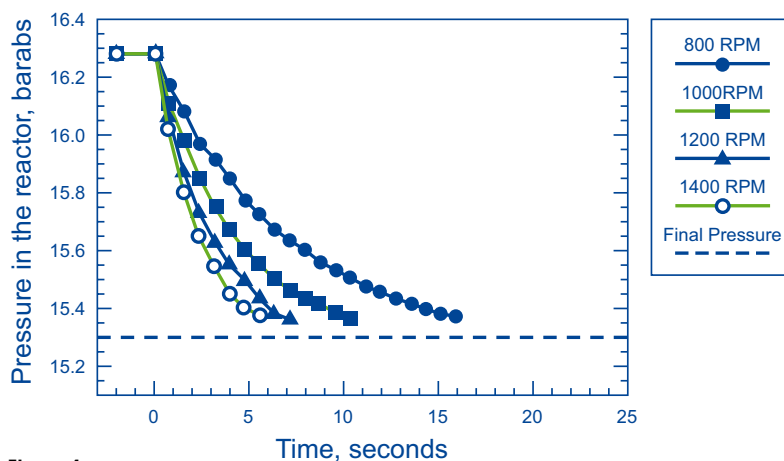

Figure 4
Pressure profile during batch hydrogen absorption in the RC1/HP60 w/induction agitator (14.3 % water in aniline @ 140 °C).
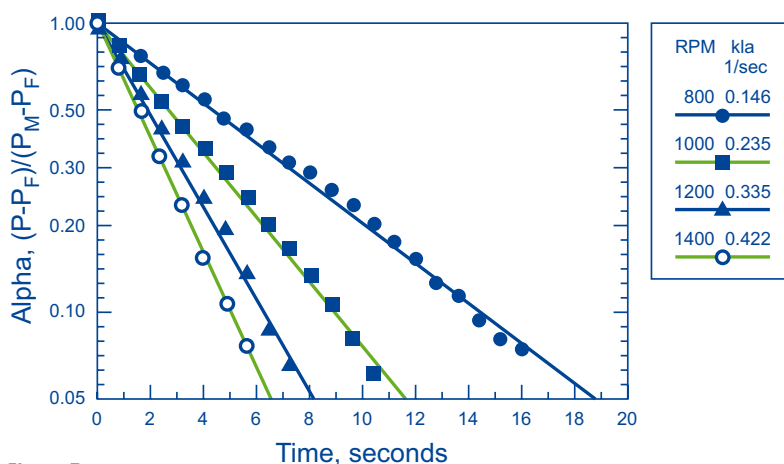

Figure 5
Characterization of gas-liquid mass transfer via batch hydrogen absorbtion (14.3 % water in aniline @ 140 °C).
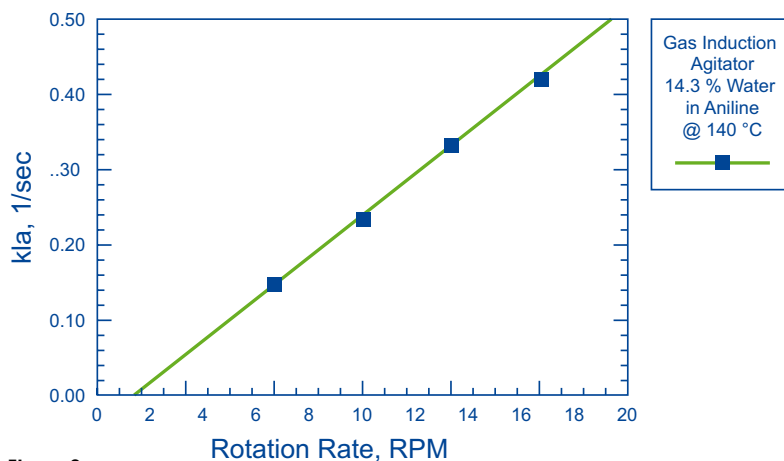

Figure 6
Effect of agitation on the gas/liquid mass transfer coefficient in the RC1/HP60.

The effect of the agitation rate on the mass transfer coefficient is plotted in Figure 6 for this reactor system. The gas mass transfer coefficient can also be a function of the liquid height above the agitator and this effect can also be studied using this technique.

However, for this study an average reactor liquid volume of 1 liter was used as a basis for comparison. In most well-designed, hydrogenation stirred tank reactors, gas mass transfer coefficients between 0.05 sec^{-1} and 0.5 sec^{-1} can be achieved.

From Figure 6, a kla of 0.235 sec^{-1} @ 1000 rpm was chosen, which represents values often found in larger-scale, stirred hydrogenation reaction vessels. Solubility measurements and estimates for a variety of conditions are tabulated in Table 1 for this study.

Hydrogen solubility in 14.3 % water/85.7 % aniline [M]			
	Total system pressure [barg]		
Temperature	8.0	11.0	14.0
140 °C	0.0090	0.0138	0.0186
160 °C	0.0073	0.0122	0.0170

Table 1
Hydrogen solubility measurements and estimates from Equation 5.

A Warning about Agitation Studies

Often it is desired to operate a laboratory reactor under conditions in which mass transfer is sufficiently fast that it does not impact the overall process hydrogenation rate. Investigators increase the agitation rate until the process kinetics no longer increase with increasing agitation. This plateau at high rotation rates is assumed to be the gas mass transfer independent region of operation. Unfortunately, this approach is not rigorous in determining if a process is independent of gas mass transfer.

Often in small reactors, especially those that are unbaffled, at high rotation rates, the process liquid begins to form a vortex and begins to swirl, limiting gas/liquid mixing and mass transfer. Under such conditions the only process that may have been elucidated is the dependency and limitation of the gas mass transfer coefficient at high agitation rates.

A more rigorous and consistent way to ensure experimentally that a process is independent of gas mass transfer is to determine the effect of changing the kla on the overall hydrogenation rate or to determine the effect of changing the catalyst concentration on the overall process rate.

For example, if changing the catalyst concentration continues to impact a process rate in a linear manner, then the process may be assumed to be independent of gas mass transfer. When gas mass transfer becomes limiting, increasing the catalyst concentration will have little or no effect on the process rate.

No experimental method is absolutely unambiguous, because catalyst concentration can also affect the mass transfer coefficient and complex reaction chemistry may vary with catalyst concentration.
It is the responsibility of the investigator to explore these variables as required.

Solid-Liquid Mass Transfer

Once hydrogen has entered the well-mixed bulk liquid phase of the stirred reactor and as feed is added to the liquid phase of the reactor, both the hydrogen and nitrobenzene, in this case, must be transported from the bulk liquid phase, according to Figure 1, to the external surface of the solid catalyst particle.
This process is designated as liquid/ solid mass transfer. When the substrate to be reduced, nitrobenzene, is in high concentration, then only the mass transfer of hydrogen needs to be considered. However, when the process is operated in a continuous or semibatch manner under conditions in which the feed is added sufficiently slowly to limit its accumulation, then its mass transport to the catalyst must be considered as well. The rate of liquid to solid mass transfer can be expressed in the following equation:

$$\text{Rate} = \frac{ks \cdot As}{V_L (C_{S, \text{bulk}} - C_{H, \text{interface}})} \qquad (8)$$

where

ks = liquid/solid mass transfer coefficient [m/sec],

As = total solid/liquid interfacial area in the reactor,

V$_L$ = reactor liquid volume,

C$_{S,bulk}$, C$_{S,interface}$ = molar concentrations of nitrobenzene or hydrogen in the bulk liquid phase and at the solid/liquid interface.

The parameters ks·As/VL can be combined into the familiar mass transfer coefficient,

$$\frac{ks \cdot As}{V_L} = ksa \qquad (9)$$

For small catalyst particles, the mass transfer coefficient, ksa [sec^{-1}], may be viewed as a fundamental parameter describing the catalyst and to a lesser extent the reactor system itself.
Unlike the kla, which is primarily a function of the agitator and reactor design, agitation intensity, and the physical properties of the fluid, the ksa in catalytic systems is often dominated by the physical characteristics of the catalyst, i.e., particle size distribution, particle shape and density.

While mixing intensity and reactor design can influence the ksa, for catalytic systems where $dp_{i,cat.}$ <50 microns, the effect of reactor design and mixing is minimal once a uniform catalyst suspension has been achieved.

The solid/liquid surface area is determined exclusively by the particle size distribution, the total amount of catalyst in the system and the catalyst density. Assuming that the catalyst particles can be approximated as spherical, the total solid/liquid surface area can be determined by summing up the surface area associated with each fraction of the particle size distribution according to the following:

$$As = \sum As_i \qquad (10)$$

$$As_i = \frac{m_{i,cat}}{\rho_{cat}} \cdot \frac{6}{dp_{i,cat}} \qquad (11)$$

where

$dp_{i,cat}$ = diameter of catalyst particle,
$m_{i,cat}$ = mass of catalyst with the particle diameter, $dp_{i,cat}$,
P_{cat} = liquid-filled catalyst density.

A number of reviews and articles describe various correlations used to estimate the liquid/solid mass transfer[14,20-22]. Most liquid/solid mass transfer correlations conform to the following relationship:

$$Sh = 2 + C \cdot Re_{pi}{}^a \cdot Sc^b \qquad (12)$$

where

Sh $ksi \cdot dp_{i,cat}/D$,
ks_i = mass transfer coefficient for particles with diameter $dp_{i,cat}$,
D = diffusivity of hydrogen or substrate in the reaction liquid mass,
Re_{pi} = particle Reynolds Number for a catalyst particle with diameter, $dp_{i,cat}$,
Sc = Schmidt Number, $\mu/(\rho \cdot D)$,
μ, ρ = liquid-phase viscosity and density, respectively,
a, b, C = dimensionless coefficients.

The theories of mass transport differ most fundamentally in their attempts to define Re_{pi} using either terminal velocity-slip velocity theory or Kolmogoroff's theory of local isotropic turbulence[20]. A complete discussion of these theories is beyond the scope of this paper and we will focus on estimates of Re_{pi} that can provide a bound on the liquid/solid mass transfer rate process. For catalyst systems with catalyst sizes less than 50 microns, often one can let C = 0 and approximate Sh = 2. This estimate is especially good with particles <10 microns. Not surprising the diffusivity is often the most critical parameter impacting estimates of the ksa so that sophisticated methods of calculating Re_{pi} are rendered futile without a reasonable measure or estimate of the diffusivity. In this system the diffusivity was estimated using the Stokes/Einstein equation which can be used when limited information is available for a system[23]. The Wilke-Chang estimation method can also be used for liquid systems[23].

$$D = 1.05 \cdot 10^{-9} \cdot \frac{T}{\mu \cdot V_m{}^{1/3}} \qquad (13)$$

where

V_m = molar volume of diffusing species at its boiling point, (113 ml/gmole for nitrobenzene, 14.3 ml/gmole for hydrogen),
T = temperature in degrees Kelvin,
μ = liquid viscosity, (0.00263 Poise @ 140 °C for 14.3 % water in aniline),
D = $3.4 \cdot 10^{-5}$ cm2/sec @ 140 °C for nitrobenzene.

Kolmogoroff's theory is based on the turbulent eddy length, λ, which is given as

$$\lambda = \left(\frac{\mu^3}{e_v \cdot \rho^2} \right)^{\frac{1}{4}} \qquad (14)$$

where

e_v = Mixing energy per unit volume of the reactor liquid reactor liquid

The Re_{pi} based on Kolmogoroff's theory is given as

$$Re_{pi} = \left(e_v \cdot dp_{i,cat}{}^4 \cdot \frac{\rho^2}{\mu^3} \right)^{\frac{1}{2}}, \text{for } \lambda \gg dp_{i,cat}$$

$$Re_{pi} = \left(e_v \cdot dp_{i,cat}{}^4 \cdot \frac{\rho^2}{\mu^3} \right)^{\frac{1}{3}}, \text{for } \lambda \ll dp_{i,cat} \qquad (15)$$

The Re_{pi} based on the terminal velocity-slip velocity is given as

$$Re_{pi} = \left(dp_{i,cat} \cdot \rho \cdot \frac{v_c}{\mu^3} \right), \quad [14] \qquad (16)$$

where

v_c = $(v_e^2 + v_{tp}^2 + v_s^2)^{1/2}$,
v_e = neutral particle relative velocity,
v_{tp} = terminal particle velocity,
v_s = slip velocity due to inertial differences between the particles and fluid.

Often for small particles we may assume for estimation purposes that $v_c = v_{tp}$.

The mass transfer coefficient for each population of the catalyst distribution is given by

$$ksa_i = ks_i \cdot As_i \qquad (17)$$

and the total mass transfer coefficient can then be calculated from

$$ksa = \sum ksa_i \qquad (18)$$

For convenience, we can define a solid/liquid mass transfer coefficient that is normalized to the weight percent of catalyst in the reaction mixture.

$$ksa = \frac{ksa}{wt\ \%\ catalyst} \qquad (19)$$

The particle size distribution for sponge nickel catalyst is illustrated in Figure 7 and is typical for this class of catalyst. In Figure 8 the partial mass transfer coefficient based on variations of Equation 12 as indicated is illustrated. The final net mass transfer coefficients for the catalyst used are tabulated in Table 2 according to Equations 17, 18 and 19. For the terminal-slip velocity theory example calculated in Table 2, the velocity, v_c, was assumed to be equal to the terminal settling velocity, v_{tp}. The terminal velocity was calculated according to Cheremisinoff[22].

Pulse Kinetic Studies
An effective way of getting a broad perspective on the kinetics in a particular system is to conduct pulse experiments with the appropriate feed under the desired conditions. It is generally easy to control temperature and pressure during pulse experiments and

a wide range of process conditions can be effectively explored. In our studies we investigated 8 barg, 11 barg and 14 barg total pressure at 100 °C, 120 °C, 140 °C and 160 °C.

Mass transfer coefficients based on a=1/2, b=1/3 according to Eqn 12.			
Normalized ksaw [1/(sec·wt % cat.)]	Basis for Re_{pi}	Mixing Energy	C, Eqn 12
0.40	———	———	0.00
0.48	Panicle terminal velocity, $v_c = v_{tp}$	———	0.72
0.61	Kolmogoroff's theory	1.0 watt/liter, agitator RC1/HP60 @ 1000, rpm w/gas	0.40
0.74	Kolmogoroff's theory	10.0 watt/liter	0.40

Table 2
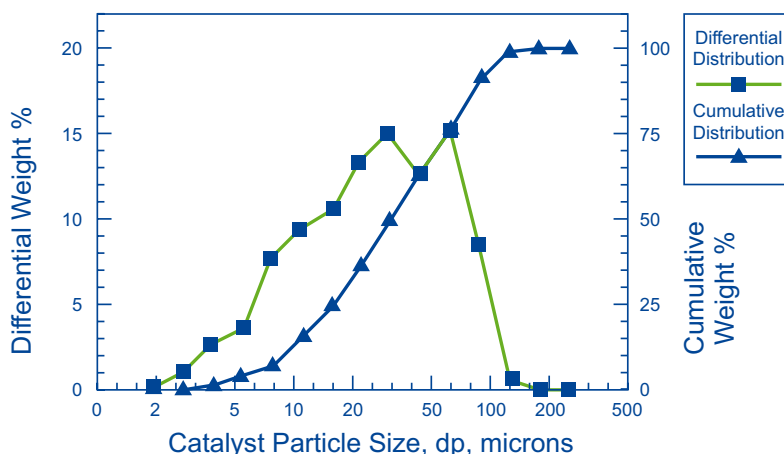Estimates of the nitrobenzene mass transfer coefficient @ 140 °C.

Figure 7
Sponge nickel catalyst particle size distribution (weight/volume average paticle size = 34.2 microns).
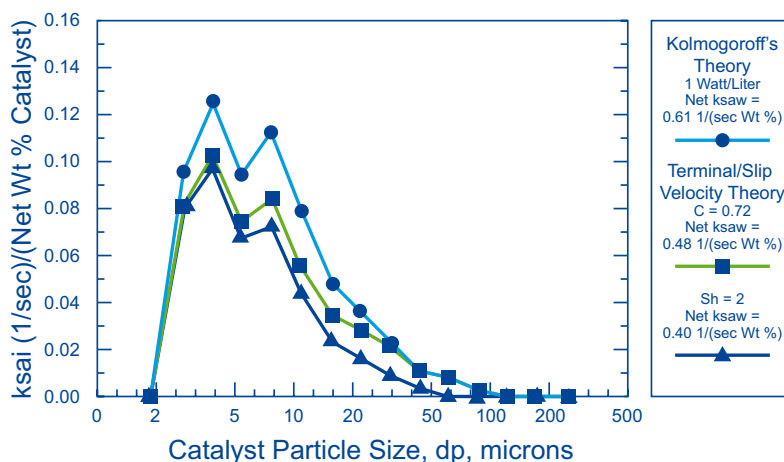

Figure 8
Comparative distributions of the mass transfer coefficient for nitrobenzene and sponge nickel catalyst.

Unlike most studies that employ hydrogen uptake as a measure of kinetics, we used isoperibolic calorimetry, i.e., the reactor jacket maintained at the designated temperature setpoint with the reaction exotherm monitored continuously in the RC1/HP60 calorimetric reactor. In this manner the hydrogen pressure can be maintained constant during the reaction.

Nominal 3 gram pulses of 50 % aniline and 50 % nitrobenzene (1500 ppm or 0.016 M nitrobenzene) were added to the reactor between 5 and 20 seconds, which contained 14.3 % water, 85.7 % aniline and approximately 0.05 % catalyst.

A sample of the isoperibolic data is illustrated in Figure 9. The data was renormalized at the end of the feed addition and conformed within statistical limits to a simple rate model, first order in nitrobenzene and zero order in hydrogen, which is illustrated in Figure 10 for experiments at 11 barg. Based on the low overall kinetic rates during the pulse tests, the complications of gas/liquid mass transfer can be ignored. The rate data was normalized for the weight percent of catalyst used and is illustrated in Table 3.

Figure 9
Exotherm profiles from feed pulse tests at 11 barg.

Figure 10
First order rate analysis of nitrobenzene pulse test
(at 11.0 barg pressure w/ 0.05 % catalyst).

Normalized first order rate constants in 14.3 % water/85.7 % aniline [1/(sec wt% cat.)]			
	Total system pressure [barg]		
Temperature	8.0	11.0	14.0
100 °C	0.117	0.0958	0.0972
120 °C	0.146	0.100	0.109
140 °C	0.467	0.482	0.567
160 °C	0.661	0.690	0.702

Table 3
Effect of temperature and pressure on nitrobenzene hydrogenation rate constants.

The rate constants are plotted according to the traditional Arrhenius model in Figure 11 and as a function of hydrogen solubility in Figure 12. There are two points that should be noted in these plots.

First, the rate constants are not a function of the hydrogen solubility as illustrated in Figure 12. Secondly, there is a sharp transition in the reaction rate constants between 120 °C and 140 °C. This transition corresponds to the transition from a single homogeneous liquid phase at 140 °C to a two-liquid-phase region at 120 °C according to Figure 3. In the single-phase region, the rate constants are a weak function of temperature and show an activation energy of 5.4 kcal/mole according to Figure 11.
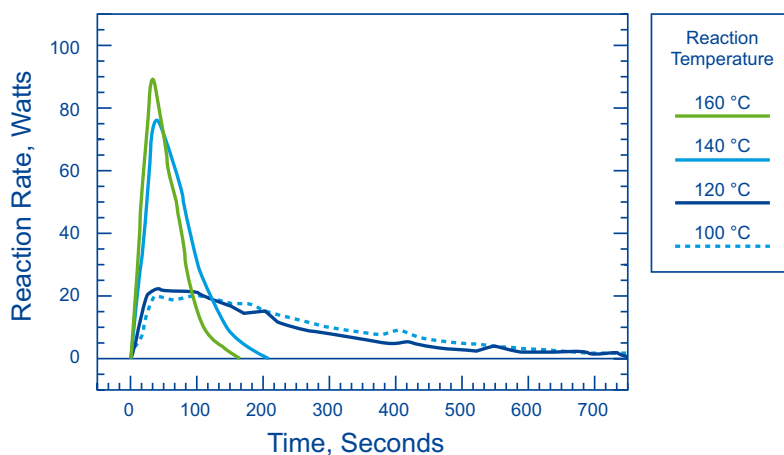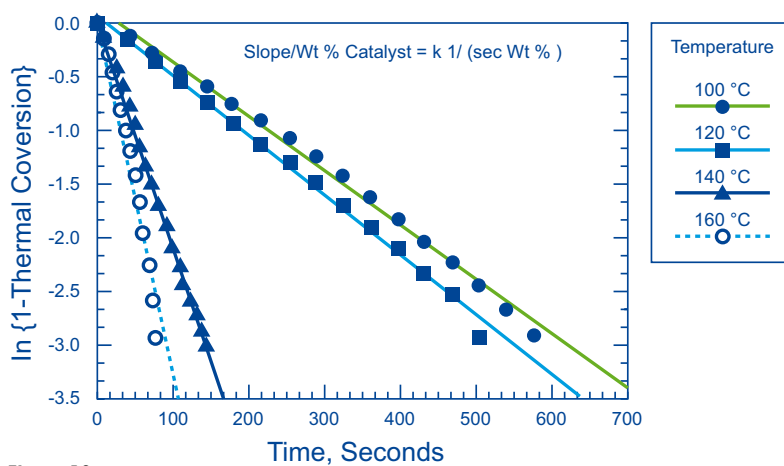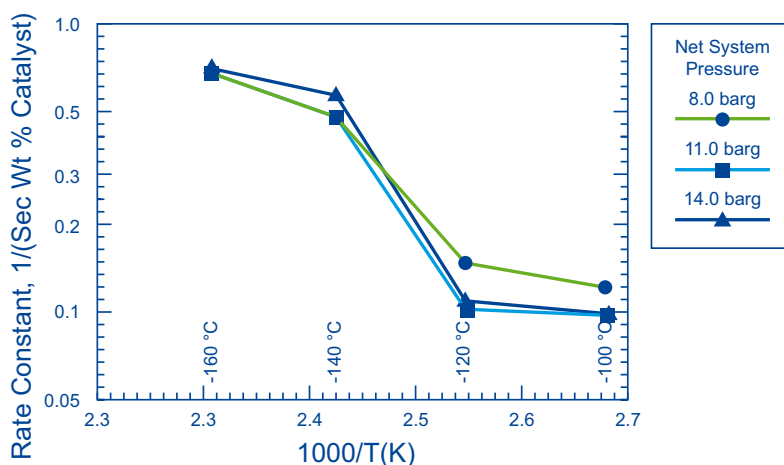

Figure 11
Arrhenius plot of normalized nitrobenzene rate constants at different pressures.

This low activation energy is consistent with mass transfer controlled processes. Recall that the normalized liquid/solid mass transfer coefficient for this catalyst given in the previous section is between 0.40 and 0.61 1/(sec · wt % cat.), which is approximately the measured rate constant at high temperature for this process.

This suggests that the process rate during the pulse experiments is controlled by liquid/solid mass transfer.

When operating under solid/liquid mass transfer control, the effective concentration of nitrobenzene at the catalyst solid/liquid interface is essentially zero, according to Equation 8. This corresponds to surface reaction kinetics that are infinitely fast compared to the time scales of diffusion.

Under the two-phase region at and below 120 °C, the rate was independent of both pressure and temperature and probably controlled by liquid/liquid mass transfer or nitrobenzene solubility limits in the water phase. Sponge nickel will generally favor the water phase in a two-phase mixture. The low rate observed in the two-phase region suggests that commercial processes should be operated under single-phase process conditions. It should also be noted that only nitrobenzene was considered to be an active species during these experiments and no other intermediates were monitored.

Semibatch and Pseudocontinuous Operation and Rate Analysis

The heat generation for highly exothermic reactions is often difficult to control in batch processes. Therefore, it is preferred to operate these reactions under semibatch or continuous addition of the feed. The overall transient mass balance for species A in a CSTR is given by the following expression for a simple process reaction, A $\longrightarrow$ B.

| Acc. | In | Out | Reaction Rate |

$$\frac{dN}{dt} = (Q_{in} \cdot C_{in}) - (Q_{out} \cdot C_{out}) - (Rate \cdot V_r) \quad (18)$$

where

N = moles of A in the reactor,

Qin, Qout = incoming and exiting volumetric flow rates to the reactor,

Cin, Cout = incoming and exiting concentration of A [moles/liter].,

Rate = volumetric molar react. rate for A $\longrightarrow$ B,

Vr = liquid reactor volume, a function of time during semibatch operation.

A reactor operated in semibatch mode requires that $Q_{out} = 0$. When a semibatch experiment is operated over a narrow volume range such that V_r(initial) and V_r(final) differ by less than approximately 20 %, then
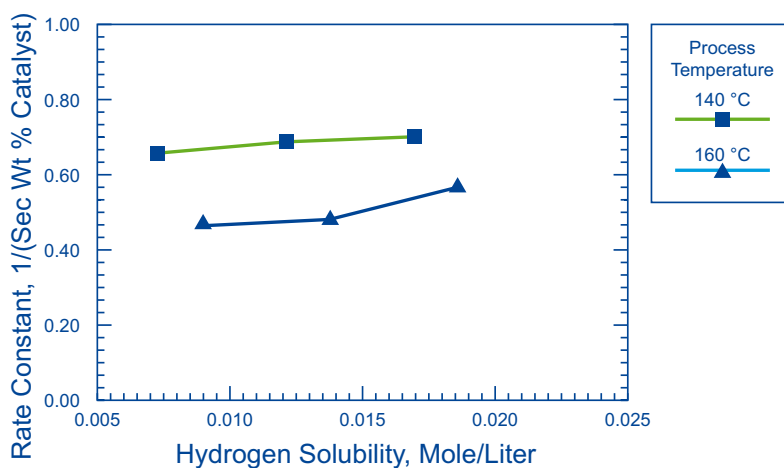

Figure 12
Effect of hydrogen concentration on normalized nitrobenzene rate constants.

the reactor volume during the semibatch experiment can be assumed constant at the average fill volume, V_r(average) = [V_r(initial) + V_r(final)]/2.

Also, if a continuous process is operated at very high conversion, then $Q_{out} \cdot C_{out} \ll Q_{in} \cdot C_{in}$ and Rate $\cdot V_r$ and $Q_{out} \cdot C_{out} \approx 0$. Then under these conditions the design equations for the continuous and semibatch processes are virtually identical:

$$\frac{dN}{dt} = (Q_{in} \cdot C_{in}) - (Rate \cdot V_r) \quad (21)$$

Since it is generally desired to operate a CSTR at high conversion, this analysis suggests that an effective method to characterize a continuous process would be operation of a semibatch process at high, instantaneous conversion, i.e., the concentration of A in the reactor $\ll C_{in}$, to obtain process results that are similar when compared to a continuous operation. This mode of operation for a semibatch reactor is called pseudocontinuous operation. From an operational perspective in the laboratory, semibatch operations yield a large volume of information using very little material and generating very little waste and are preferred over true continuous operation whenever possible.

The application of this concept is best illustrated in Figure 13. The RC1/HP60 reactor was filled to approximately 1 liter with 14.3 % water, 85.7 % aniline and 0.5 grams of catalyst. Six consecutive increasing feed ramps of 50 % aniline/50 % nitrobenzene were imposed. The reaction was run at 140 °C at 14.0 barg. Two curves are illustrated in Figure 13. The first shows the theoretical maximum exotherm rate based on the feed rates assuming that the reaction rate is infinite and the second curve is the actual reaction rate measured in watts.

As illustrated, during the first three feed ramps, the reaction rate initially trailed the step changes in the feed rate but eventually approached so that at the rate plateaus, $Q_{in} \cdot C_{in} = Rate \cdot V_r$. During these first three step changes, accumulation of nitrobenzene was minimal and the semibatch reactor was operating in pseudocontinuous mode.

Note that the ksa estimated for this process is ksa = 0.5 1/(sec · wt % cat.) · 0.05 % catalyst = 0.025 (1/sec). This is one order of magnitude smaller than the kla = 0.235 1/sec.

Figure 14 illustrates the concentration profiles of two intermediate species, azoxybenzene and azobenzene, and nitrobenzene. During the first three steps in feed, the only species identified was nitrobenzene. This result is consistent with the first path of the Haber reaction scheme, illustrated in Figure 2, and yields high reaction rates when the feed is added continuously to maintain the nitrobenzene at low concentrations, < 0.1 %. It is also consistent with the pulse test experiments, which demonstrate that under low nitrobenzene concentration the rate processes are controlled by liquid/solid mass transfer.

As the feed ramps continue, the reaction rate begins to deviate significantly from the theoretical rate based on the feed rate. As the rate of nitrobenzene addition increases, the reaction rate decreases and the accumulation of nitrobenzene in the reactor increases dramatically. As the rate decreases with increasing nitrobenzene concentration, the emergence of azoxybenzene is revealed in Figure 14. At this point the process no longer conforms to pseudocontinuous operation and the reaction mechanism begins to shift to the second pathway described by Haber illustrated in Figure 2.
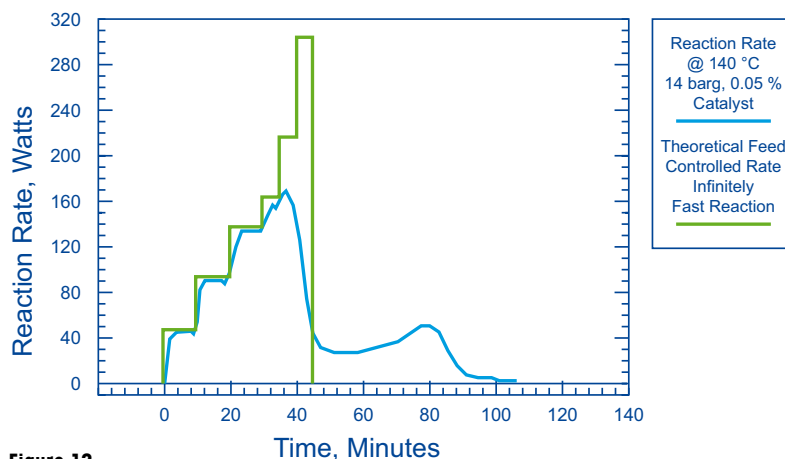

Figure 13
Effect of feed rate on reaction rate during multiramp feed experiments: comparison with theoretical feed controlled rate.
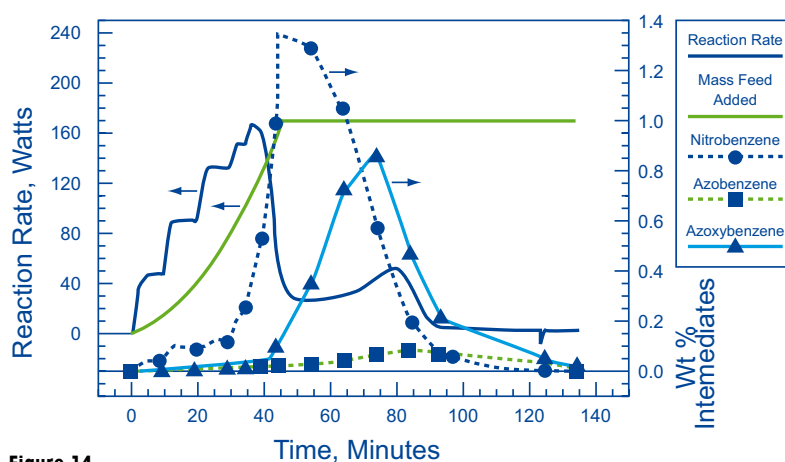

Figure 14
Accumulation of nitrobenzene and formation of intermediates (140 °C, 14 barg, 0.05 % catalyst).

The process rate as a function of nitrobenzene concentration is illustrated in Figure 15 for the range of operation before the appearance of intermediates. This analysis is similar to that of Lopidana[2] who investigated the hydrogenation of nitrobenzene on platinum catalysts. He shows that the linear portion of the rate curve at low nitrobenzene concentration is zero order with respect to hydrogen, as found in this study during the pulse tests. In addition, he demonstrated that the plateau region of the rate curve is obviously zero order with respect to nitrobenzene, yet first order with respect to hydrogen.

The process rates, calculated using Equation 22, from the pulse experiments at 140 °C and 14 barg are plotted in Figure 15. The rates are identical with those observed from the pseudocontinuous operation at low nitrobenzene concentration. This demonstrates that under the pseudocontinuous operation, the reactor is operating under liquid/solid mass transfer control.

Calculation of rates from the pulse experiments:

$$\text{Rate [watts]} = -\Delta H_{reaction} \text{ [J/mole]} \cdot k \text{ [sec}^{-1} \cdot \text{wt \%cat}^{-1}]$$
$$\cdot V_r \text{ [liter]} \cdot C_{nitrobenzene} \text{ [M]} \tag{22}$$

Note: 0.100 % nitrobenzene @ 140 °C = 0.00813 M
where

$\Delta H_{reaction}$	= Heat of reaction based on nitrobenzene (-536.6 ± 5.9 kJ/mole).
$k(\text{sec}^{-1} \cdot \text{wt \% cat.}^{-1})$	= Process rate constants from pulse experiments.

Eventually, the feed is stopped for the run in Figures 13 and 14 and the process rate achieves a new yet much lower overall value. At this point the reactor is operating in a «batch» mode. The low rate is apparently caused by the affinity of nitrobenzene, azoxybenzene and perhaps azobenzene for the catalyst and their competition with hydrogen for surface sites. This «poisoning» of the catalyst by process intermediates and nitrobenzene must be avoided to maintain high production rates. Not until the concentrations of nitrobenzene and the intermediates have been reduced does the rate begin to recover, increasing at the end of the process.

Without the sensitive measurements of the heat generation curves, the overall reaction rates observed in this regime may appear to be constant using conventional rate measurement techniques. This may explain why many investigators report that under batch conditions at constant pressure, the reaction order is zero with respect to nitrobenzene or conversion. From the heat generation curves and concentration profiles, this conclusion is obviously an oversimplification of the rate process. These lower process rates at high nitrobenzene concentration indicate that the process has changed from liquid/solid mass transfer control to a more complex, mixed control regime impacted most likely by adsorption, interparticle mass transfer and surface kinetics.
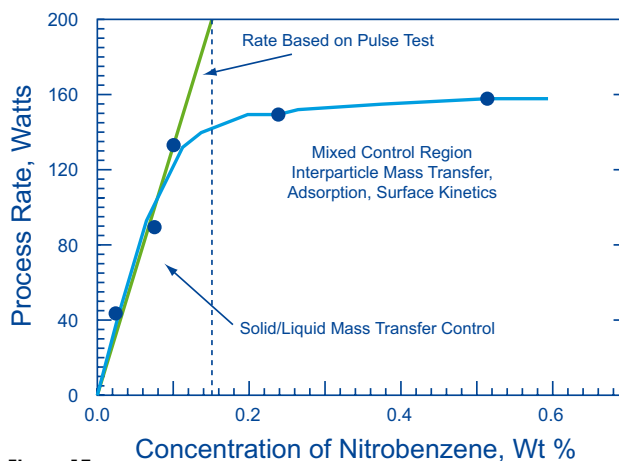

Figure 15
Effect of nitrobenzene concentration on overall process rate (140 °C, 14 barg, 0.05 % catalyst).

Scale-up Calculations

The maximum process rates may be estimated for a variety of simplified cases. For example, the maximum rate based on the gas mass transfer assumes that the bulk hydrogen concentration is equal to zero. Although this situation is generally not desired in a real process, it does give an upper limit on the maximum rate possible in a reactor system based on the gas mixing. We can define the Maximum Gas Mass Transfer Rate, MGMTR, as

$$MGMTR = kla \cdot CH_{2,sat} \tag{23}$$

In our system, at 140 °C and 1000 rpm,
MGMTR = 0.235 sec^{-1} · 0.0186 M,
MGMTR = 0.00437 moles hydrogen/(liter · sec).

In terms of reactor energy production,

$$MGMTR = kla \cdot CH_{2,sat} \cdot \text{ß}{-}1 \cdot -\Delta H_{reaction} \tag{24}$$

where

ß	= Stoichiometric factor, moles hydrogen/ moles substrate (ß = 3 for nitrobenzene).
MGMTR	= 782 watts/liter in this study at 140 °C at @ 1000 rpm.

The hydrogen in the bulk phase during the reaction can be calculated by combining Equations 3 and 23 to get the following:

$$CH_{2,bulk} = CH_{2,sat} \cdot (1{-}\text{Rate/MGMTR}) \tag{25}$$

Consider operating the reduction of nitrobenzene in a large-scale reactor continuously with sufficient catalyst and feed rate to give a steady-state energy production

rate of 300 watts/liter. If the reactor has a MGMTR of 600 watts/liter as calculated from Equation 23, then the hydrogen concentration in the bulk at steady-state can be estimated to be half of the saturation concentration based on Equation 25. To operate a laboratory reactor at the same bulk hydrogen concentration conditions, either the pressure, the mass transfer coefficient or both must be adjusted according to equation 25 to match so that the following condition is met:

$$CH_{2,sat,1} \cdot (1\text{-}Rate_1/MGMTR_1) = \qquad (26)$$
$$CH_{2,sat,2} \cdot (1\text{-}Rate_2/MGMTR_2)$$

where the subscript 1 designates the scaled-up reactor at pressure P1 and subscript 2 designates the laboratory reactor at P2.

To achieve similar catalyst interfacial concentrations of hydrogen and nitrobenzene in both the laboratory reactor and the plant reactor, the reactor should be operated at the same volumetric production rate and catalyst concentration. As long as the bulk hydrogen concentrations in both reactors are the same, then the concentration profiles in the large reactor and the laboratory will be equivalent.

Example:
It is desired to operate a large scale-up CSTR at 500 watts/liter, which corresponds to an aniline production rate of 0.932 moles aniline/(m^3·sec) or 0.000932 moles aniline/(liter · sec).
The reactor is operated continuously at 140 °C, 8 barg, with a volume of 1 m^3, a kla of 0.5 sec^{-1} and a feed of 50 % aniline/50 % nitrobenzene. Calculate the bulk hydrogen concentration and the required catalyst.

The MGMTR is calculated from Equations 23 and 24:
MGMTR = 0.5 sec^{-1}·0.0090 M
     = 0.0045 moles hydrogen/(sec liter)
MGMTR = 0.0045 moles hydrogen/(sec·liter)/3
     · 536,600 J/mole nitrobenzene
     = 805 watts/liter
$CH_{2,bulk}$ = (1−500/805) · 0.0090 M = **0.0034 M**

To maintain operation in the low nitrobenzene range, we chose to operate at 0.05 wt % or 0.004065 M nitrobenzene in the reactor.
The process rate constant in this region of operation is 0.467 sec^{-1} · wt % cat.$^{-1}$, according to Table 3.

The catalyst requirement can be calculated:
wt% catalyst = 0.000932 moles aniline/
      (liter·sec)/(0.467 sec^{-1} · wt % cat.$^{-1}$
      · 0.004065 M nitrobenzene)
      = **0.49 %**

Conclusions
The hydrogenation of nitrobenzene is a complex process impacted by the competing effects of mass transfer and kinetics. These processes, however, can be individually analyzed to reveal the controlling mechanisms under different process conditions. The reaction pathway according to Haber is determined by reactor process conditions. At high temperature and low nitrobenzene concentration, solid/liquid mass transfer was found to dominate, yielding a process that could be operated at high rates. However, at higher nitrobenzene concentration intermediates form, which along with nitrobenzene poison the catalyst and lead to low process rates.

References
1. McMurry, J., Organic Chemistry, Brooks/Cole Publishing Company, Monterey, Calif., p. 961 (1984).
2. Rihani, D.N., T.K. Narayanan and L.K. Doraiswamy, «Kinetics of Catalytic Vapor Phase Hydrogenation of Nitrobenzene to Aniline» I&EC Process Design and Development, Vol. 4, No. 4, pp. 403-410 (1965).
3. Loppidana, M.A.A., et al., «Hydrogenation of Aromatic Nitro Compounds with a Pt/SiO2-AlPO4 Catalyst» Bull. Chem. Soc. Jpn., 60, pp. 3415-3419 (1987).
4. Schorlemmer, C., «Reaction Kinetics of Hydrogenation of Nitrobenzene to Aniline in the Liquid Phase» Chem. Techn., Vol. 33, No. 1, pp. 24-28 (1981).
5. Yao, H.C., and P.H. Emmett, «Kinetics of Liquid Phase Hydrogenation. II. Hydrogenation of Aromatic and Aliphatic Nitrocompounds Over a Colloidal Platinum Catalyst» J. Am. Chem. Soc., Vol. 83, pp. 796-799 (1961).
6. Yao, H.C., and P.H. Emmett, «Kinetics of Liquid Phase Hydrogenation. II. Hydrogenation of Aromatic and Aliphatic Nitroconpounds Over a Colloidal Platinum Catalyst» J. Am. Chem. Soc., Vol. 83, pp. 796-799 (1961).

References

7. Yücelen, F., Thesis Dissertation, Effects of Mass Transfer in Liquid Phase Catalytic Consecutive Hydrogenation of 2,6-Dinitrotoluene, Swiss Federal Institute of Technology, Zürich (1984).

8. Smith, G.V., R. Song, M. Gasior, R.E. Malz, Jr., «Hydrogenation of Nitrosobenzene Over Palladium Catalysts» Preprints of Pagers and Posters of the 14th Conference on Catalysis of Organic Reactions, edited by J. R. Kosak and T. A Johnson, Albuquerque, New Mexico, April 27-29, 1992.

9. Mettler Toledo Inc., 69 Princeton-Heightstown Rd., P.O. Box 71, Heightstown, N.J. 08520-0071.

10. Strätz, A. M., Catalysis of Organic Reactions, Vol. 18, Chapter 17, p. 337, Dekker (1984).

11. Campbell, A. N., L Am. Chem. Soc., 67, pg. 981 (1945).

12. Alexejew, W., Ann. Phvs. (Leipzig), Neue Folge 28, pg. 305 (1886).

13. Tatterson, G.B., Fluid Mixing and Gas Dispersion in Agitated Tanks, McGraw-Hill, New York (1991).

14. Ramachandran, P.A., and R.V. Chaudhari, Three-Phase Catalytic Reactors, Topics in Chemical Engineering, Vol. 2, Chapters 9, Gordon and Breach Science Publishers, Philadelphia (1983).

15. Yagi, H., and F. Yoshida, «Gas Absorption by Newtonian and Non-Newtonian Fluids in Sparged Agitated Vessels», Ind. Eng. Chem. Process Des. Dev., Vol. 14, No. 4 (1975).

16. Yoshida, F., and K. Akita, «Performance of Gas Bubble Columns: Volumetric Liquid Phase Mass Transfer Coefficient and Gas Hold-up», AIChE Journal, Vol. 11, No. I (1965).

17. Kato, Y., et al., «Gas Holdup and Overall Volumetric Absorption Coefficients in Bubble Columns with Suspended Solid Particles. Absorption Rate of Oxygen by an Aqueous Solution of Sodium Sulfite», Intenrnational Chemical Engineering, Vol. 13, No. 3 (1973).

18. Murugesan, T., and T. E. Degaleesan, «Hold-up, Interfacial Area and Power Requirements in Turbine Agitated Gas-Liquid Contactors», Chem. Eng. Comm., Vol. 117. pp. 263-278 (1992).

19. Dietrich, E., C. Mathieu, H. Delmas and J. Jenck, «Raney-Nickel Catalyzed Hydrogenations: Gas-Liquid Mass Transfer in Gas-Induced Stirred Slurry Reactors», Chemical Engineering Science, Vol. 47, No. 13/14 (1992).

20. Nienow, A.W., Mixing in the Process Industries, Butterworths Series in Chemical Engineering, Chapter 18, London (1985).

21. Beenackers, A.A.C.M., and W.P.M. Van Swaaij, «Mass Transfer in Gas-Liquid Slurry Reactors» Chemical Engineering Science, Vol. 48, No. 18, pp. 3109-3139 (1993).

22. Cheremisinoff, N.P., (Editor), Encyclopedia of Fluid Mechanics, Vol. 5, Slurry Flow Technology, Gulf Publishing Company, Houston, pp. 685-716 and pp. 197-209 (1986).

23. Reid, R.C., J.M. Prausnitz and T.K. Sherwood, The Properties of Gases and Liquids, 3rd ed., McGraw-Hill Book Company, New York, pg. 567 (1977).

This lecture was held at the 7th RC User Forum USA in St. Petersburg Beach, Florida, in October 1994.

www.mt.com/AutoChem

For more Information

Quality certificate. Development, production and testing according to ISO 9001.

Environmental management system according to ISO 14001.

European conformity. The CE conformity mark provides you with the assurance that our products comply with the EU directives.